Electronic Supplementary Material (ESI) for Journal of Materials Chemistry B.

Supporting Information:

Physiochemical properties and bioapplication of nano- and microsized hydroxy zinc phosphate particles modulated by reaction temperature

Peng Liu[a,b], Bangshang Zhu[*a], Xiaoya Yuan[a], Gangsheng Tong[a], Yue Su[b], and Xinyuan Zhu[b]

[a] Instrumental Analysis Center, Shanghai Jiao Tong University, Shanghai 200240, P. R. China

[b] School of Chemistry and Chemical Engineering, State Key Laboratory of Metal Matrix Composites, Shanghai Jiao Tong University, Shanghai 200240, P. R. China

* bshzhu@sjtu.edu.cn

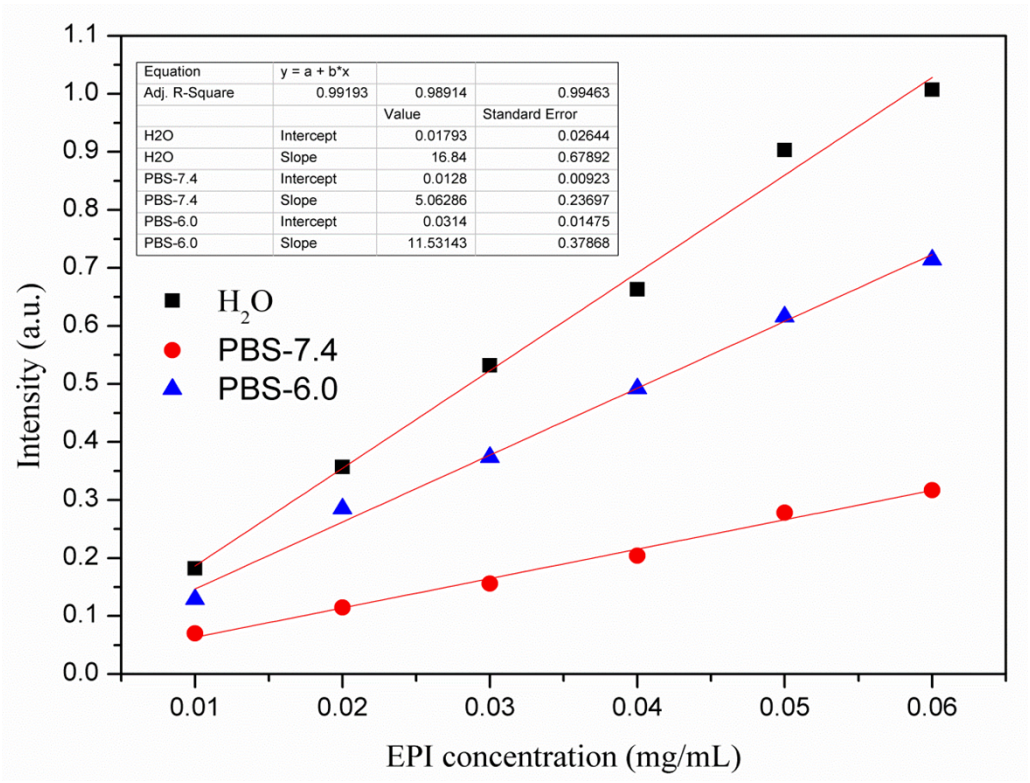

Fig. S1. The standard curve of the UV-Vis absorbance of EPI in water, PBS solution with pH value of 6.0 and 7.4.

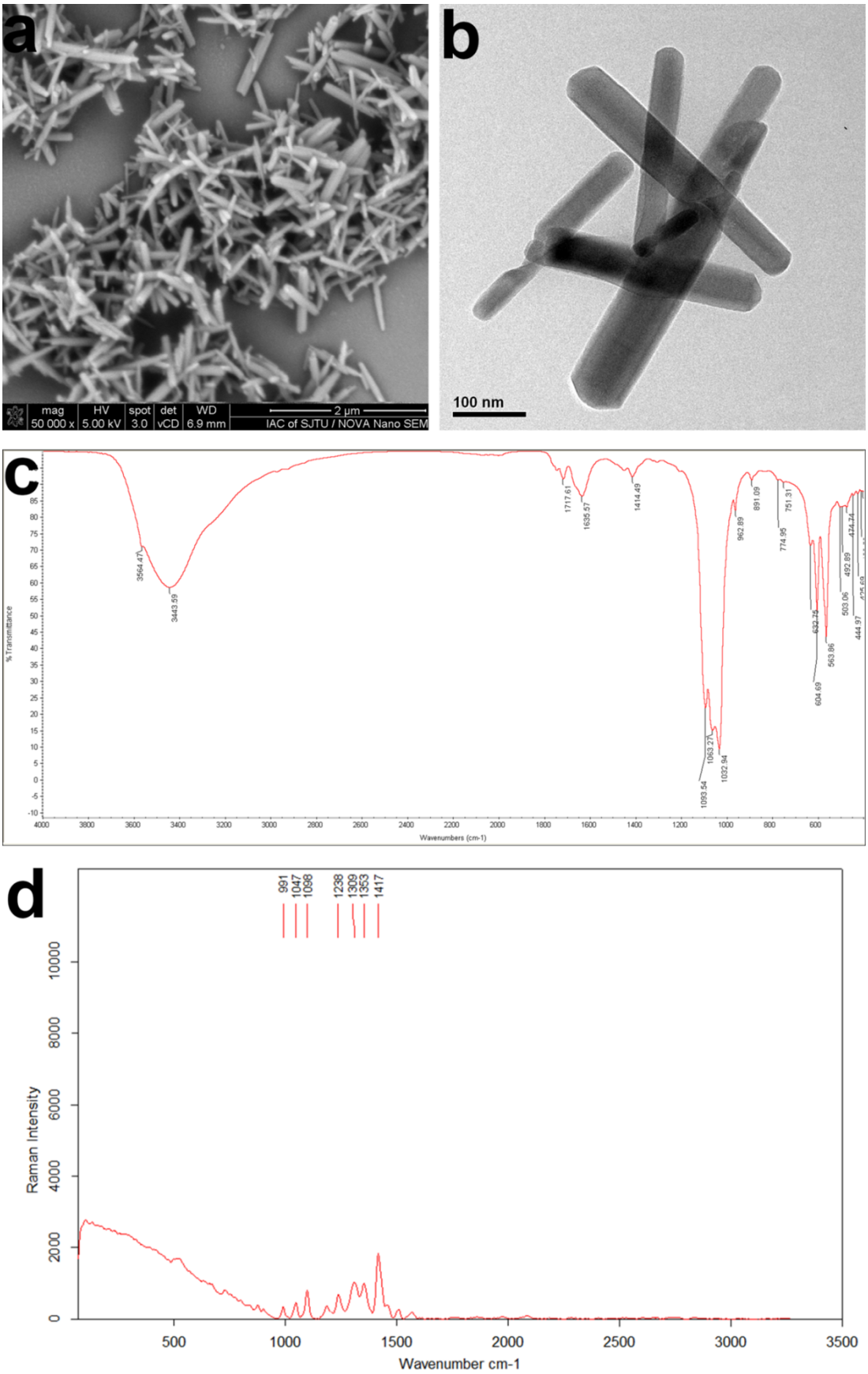

Fig. S2. The morphological and viberational characteristics of hydroxyapatite (HA). (a) SEM investigation; (b) TEM investigation; (c) FTIR spectrum; (d) Raman spectrum.

Hydroxyapatite fabrication:

To synthesize pure hydroxyapatite, 75 mL $Ca(NO_3)_2$ (33.4 mM) and 0.4 mL ammonia (25-28%) solution were added into a 250 mL flask. 1,1,1-Tris(hydroxyl methyl) ethane was used as surfactant additive and added with 1 wt% into the flask before the experiment. The reaction temperature was controlled at 90 °C and the mixture was stirred magnetically for a few minutes until 1,1,1-tris(hydroxyl methyl) was fully dissolved. Then 50 mL $(NH_4)_2HPO_4$ (20 mM) solution was slowly added dropwise to this solution, with continuous stirring. The solution was stirred at 90 °C for a further 24 h, and then allowed to stand overnight, after which the product was collected by centrifugation and ultrasonic washing with ultrapure water to neutral, and followed by lyophilisation.

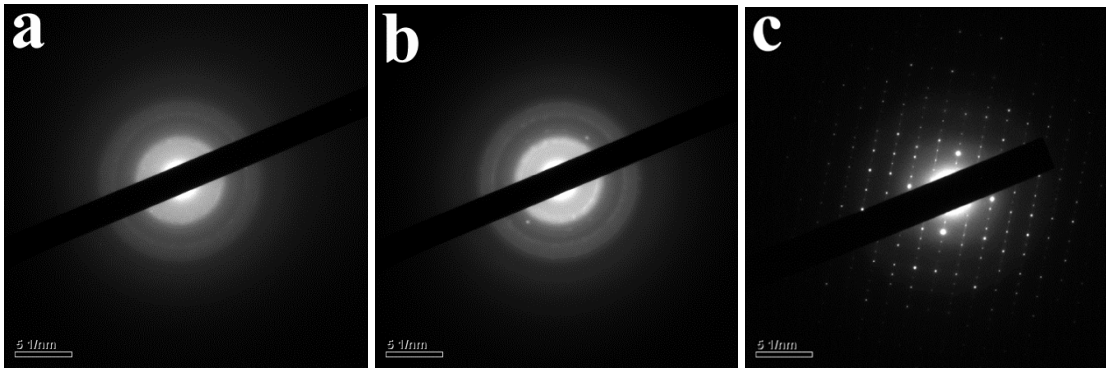

Fig. S3. The selected-area electron diffraction (SAED) pattern of HZnPPs synthesized at (a) 20, (b) 35 and (c) 65 °C, respectively.

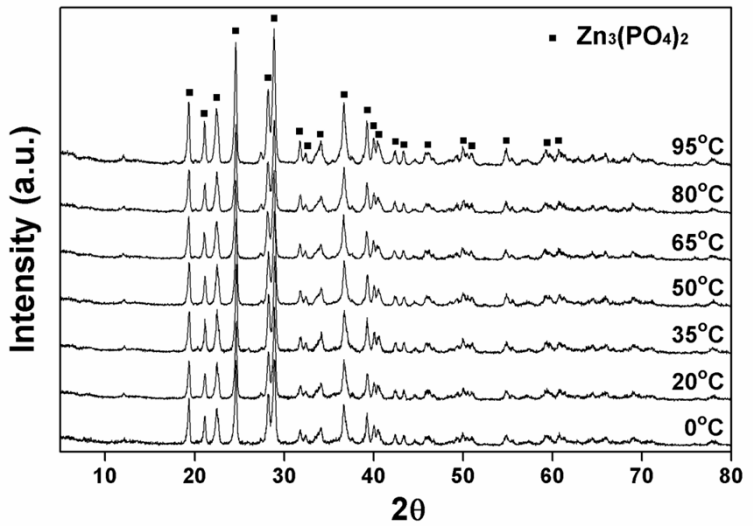

Fig. S4. XRD patterns of the HZnPPs (synthesized at 0, 20, 35, 50, 65, 80 and 95 °C) after calcination at 600 °C for 1 h. All peaks of the samples after heat treatment match well with that of $Zn_3(PO_4)_2$ (PDF:29-1390)

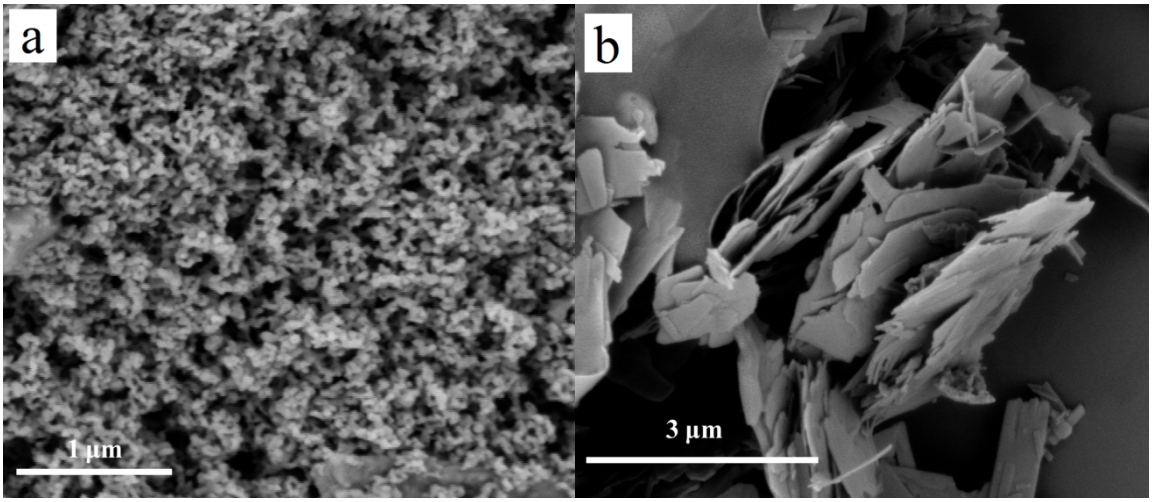

Fig. S5. The SEM investigation of the size and morphology of HZnPPs synthesized at (a) 50 and (b) 80 °C, respectively.

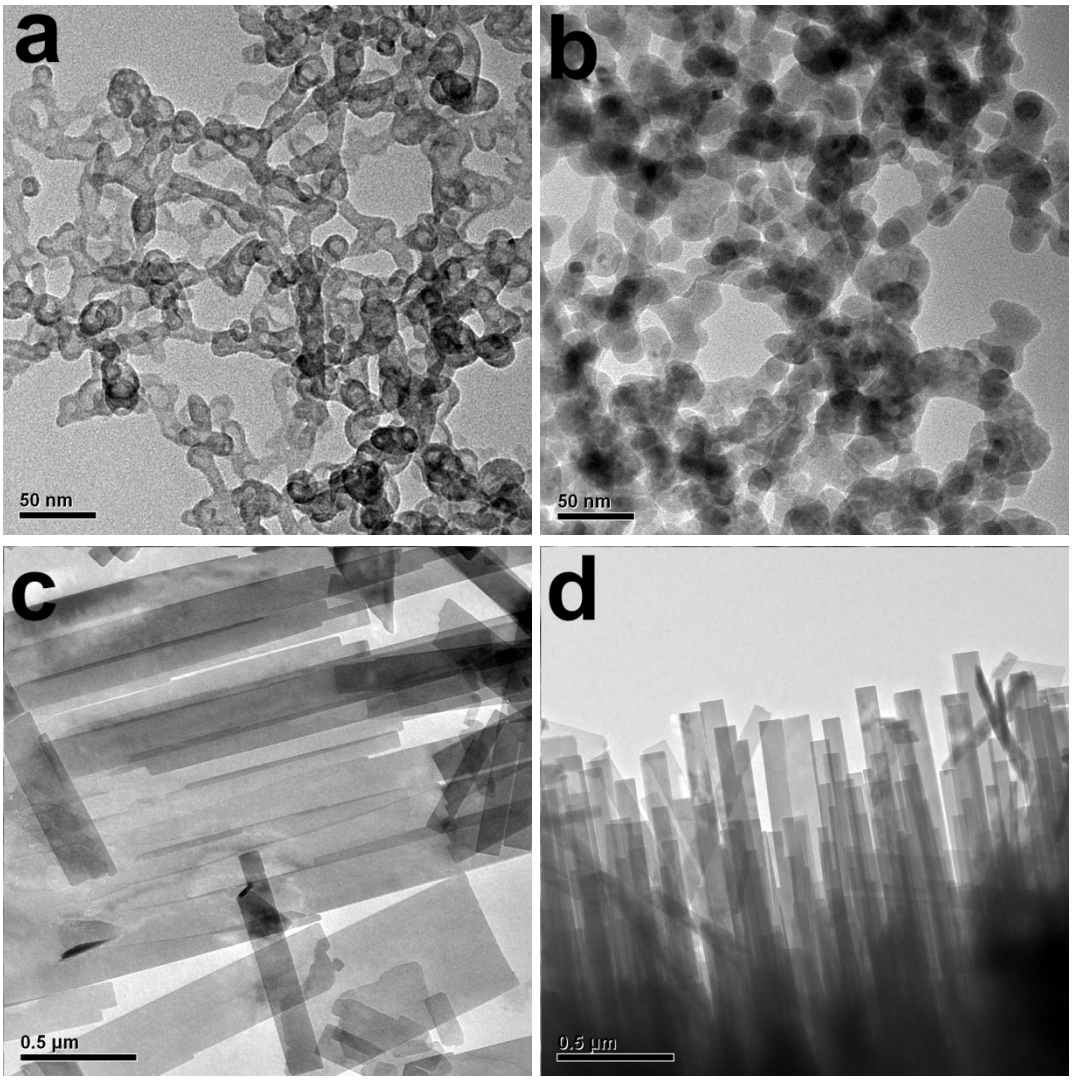

Fig. S6. The TEM investigation of the size and morphology of HZnPPs synthesized at (a) 0, (b) 50, (c) 80 and (d) 95 °C

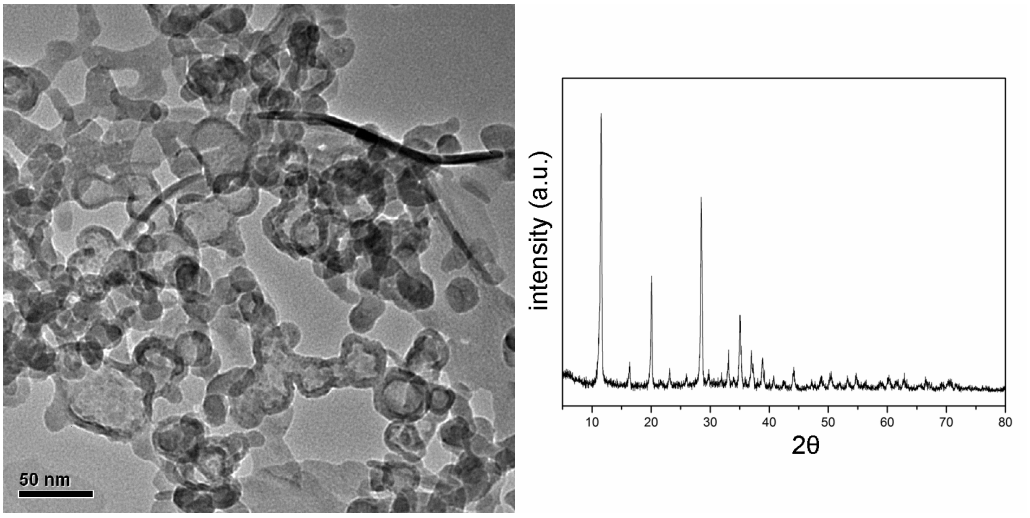

Fig. S7. The TEM observation and XRD pattern of HZnPPs synthesized at 20 °C without TME. It shows that the HZnPPs synthesized at 20 °C in the absence of TME also have the same hollow structure and XRD pattern as the previous samples. The XRD analysis result indicates that TME does not affect the crystallinity of the material.

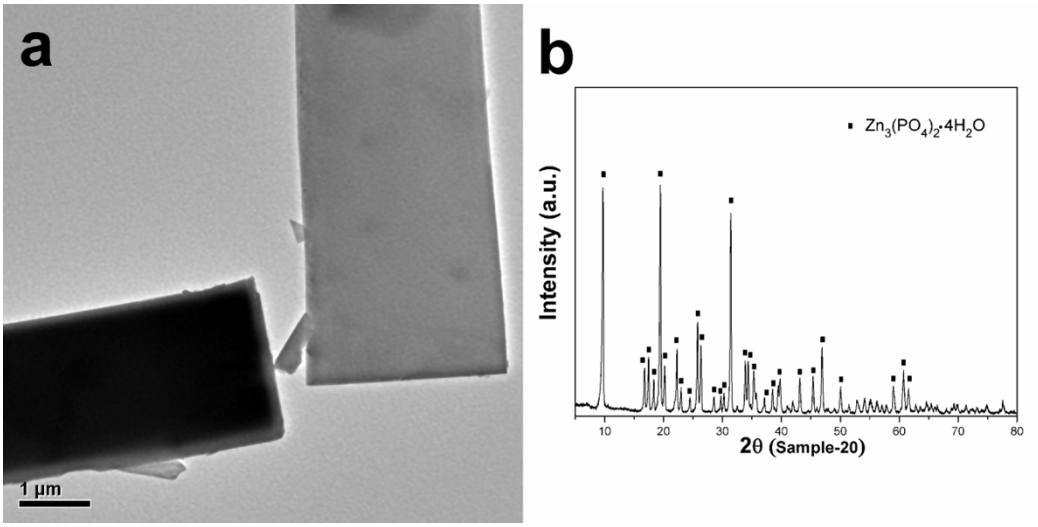

Fig. S8. The obtained materials without ammonia added in the synthesis process. (a) The TEM investigation; (b) The XRD analysis.

The material obtained by wet-chemical precipitation of $Zn(NO_3)_2 \cdot 6H_2O$ and $(NH_4)_2HPO_4$ without ammonia added (neutral). The reaction temperature was controlled at 20 °C. The material was analyzed with TEM and XRD investigation. The particles obtained are micro-scale in size and rectangle plate in shape. The particle morphology is completely different from the hollow zinc hydroxyl apatite. Furthermore, the XRD analysis shows it is well matched with $Zn_3(PO_4)_2 \cdot 4H_2O$ (PDF: 37-0465).

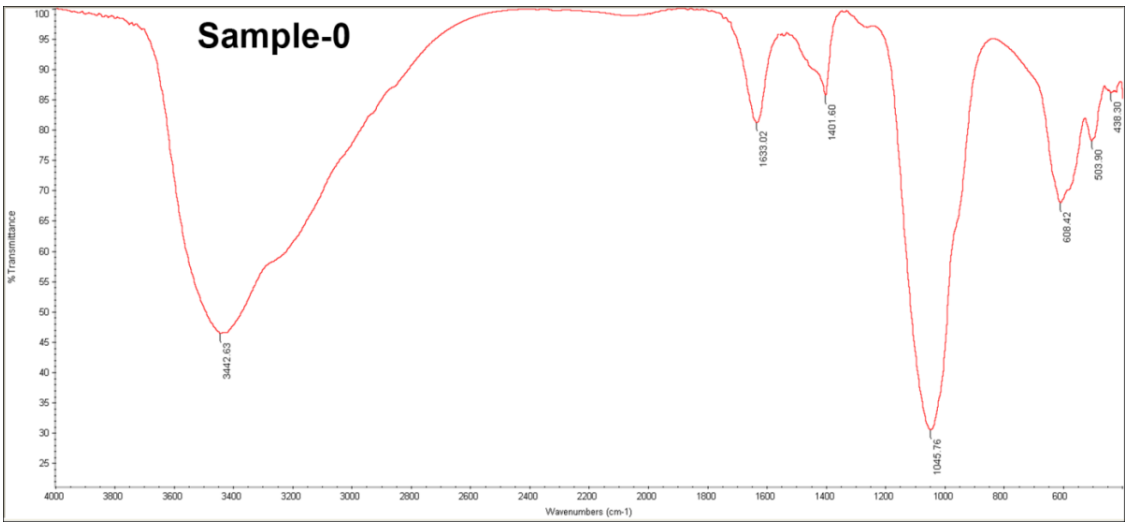
Sample-0
% Transmittance
Wavenumbers (cm-1)
3442.63
1633.02
1401.60
1045.76
608.42
503.90
438.30

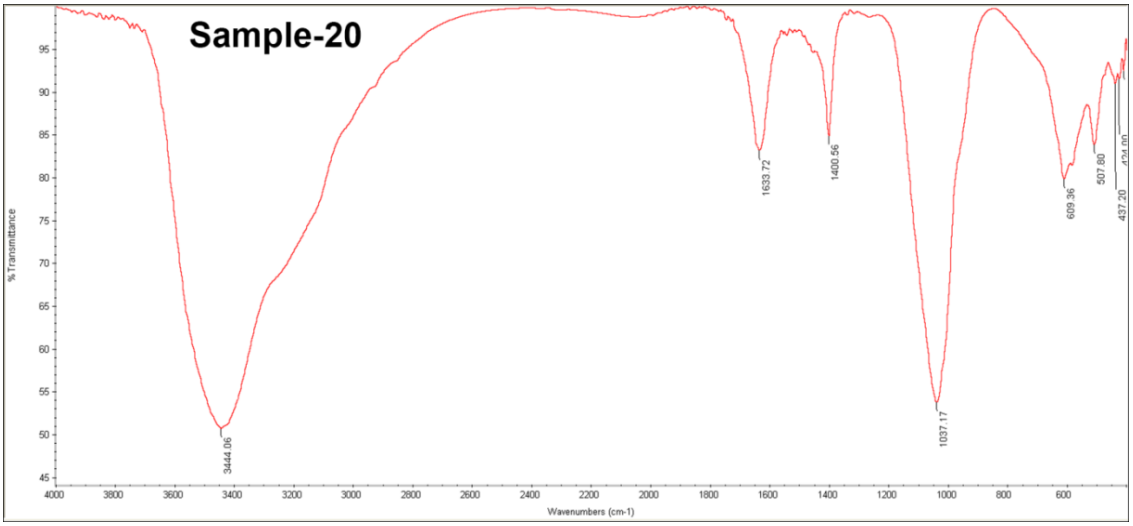
Sample-20
% Transmittance
Wavenumbers (cm-1)
3444.06
1633.72
1400.56
1037.17
609.36
507.80
437.20

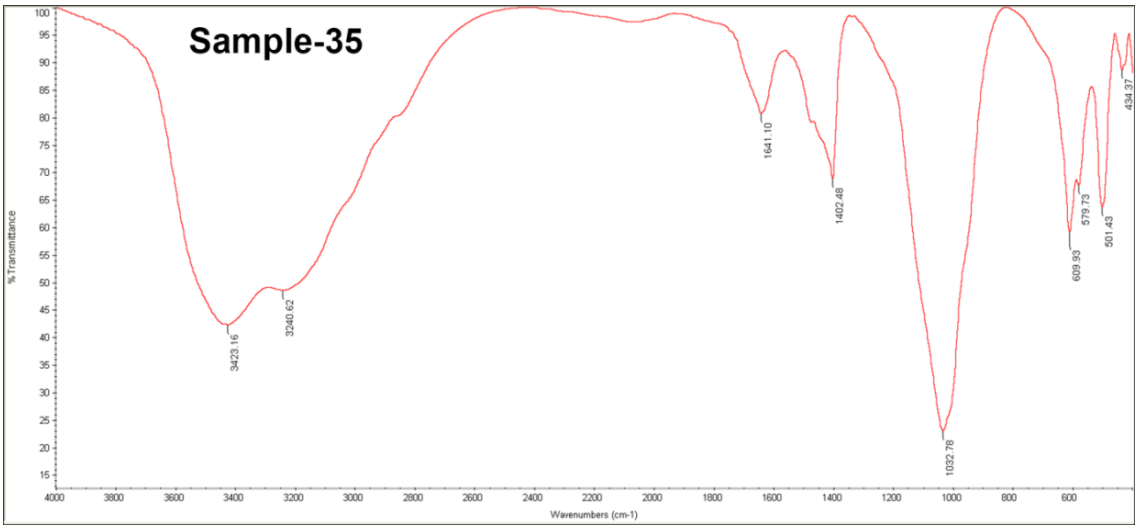
Sample-35
% Transmittance
Wavenumbers (cm-1)
3423.16
3240.62
1641.10
1402.48
1032.78
609.93
579.73
501.43
434.37

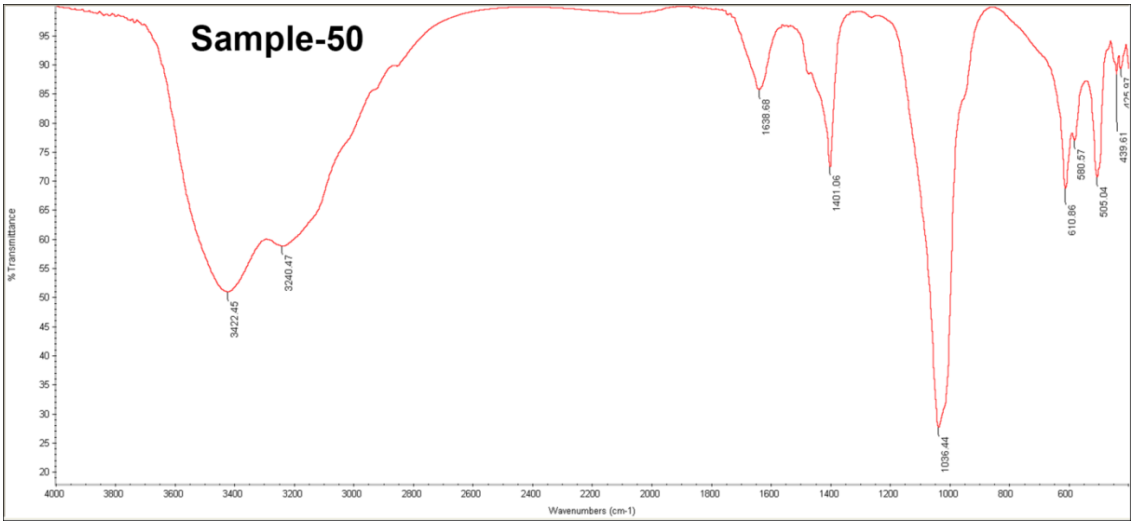
Sample-50
% Transmittance
Wavenumbers (cm-1)
3422.45
3240.47
1638.68
1401.06
1036.44
610.86
580.57
505.04
439.61

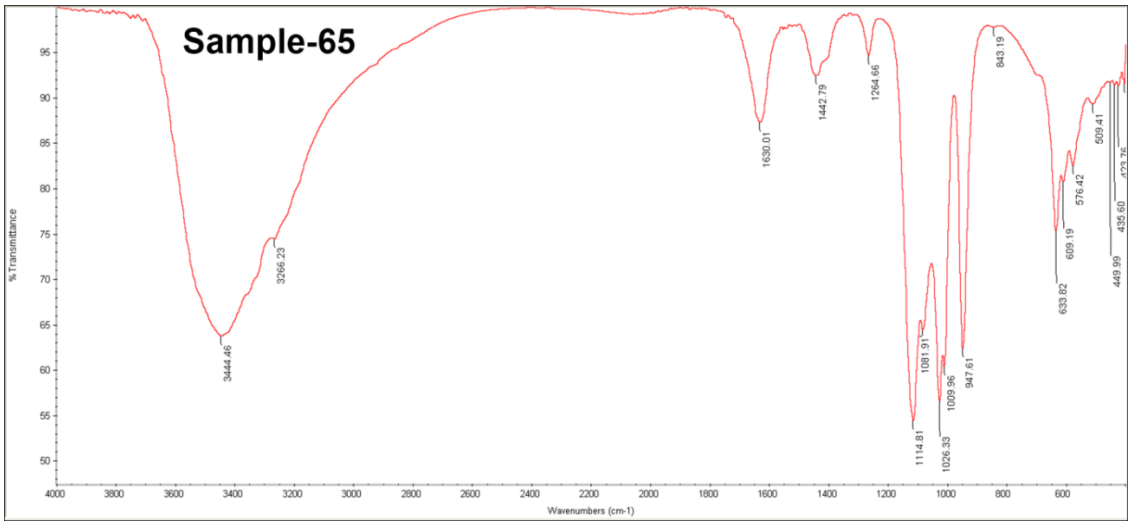
Sample-65
% Transmittance
Wavenumbers (cm-1)
3444.46
3266.23
1630.01
1442.79
1264.66
1114.81
1081.91
1026.33
1009.96
947.61
843.19
633.62
609.19
576.42
509.41
449.99
435.60

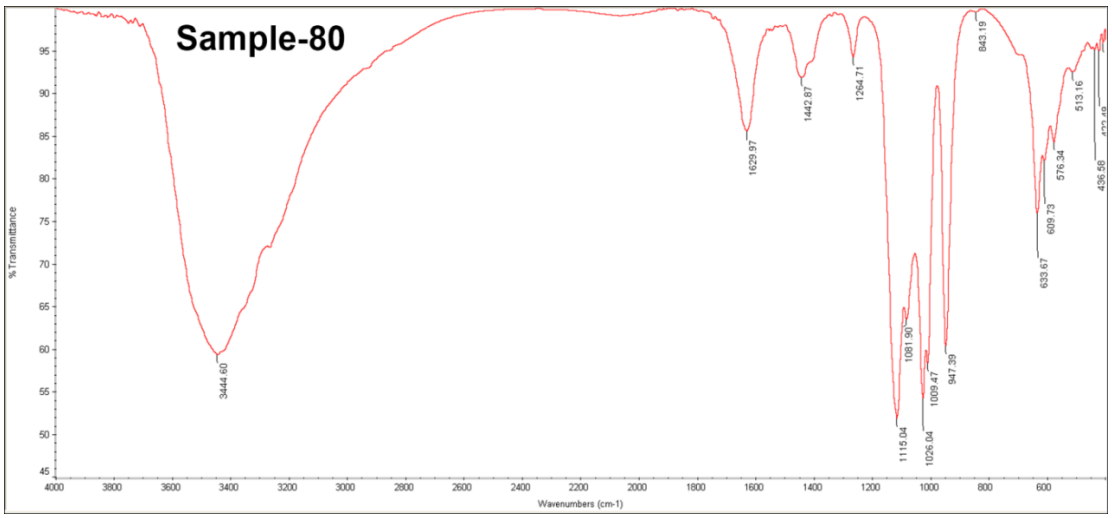
Sample-80
% Transmittance
Wavenumbers (cm-1)
3444.60
1629.97
1442.87
1264.71
1115.04
1081.90
1026.04
1009.47
947.39
843.19
633.67
609.73
576.34
513.16
436.68

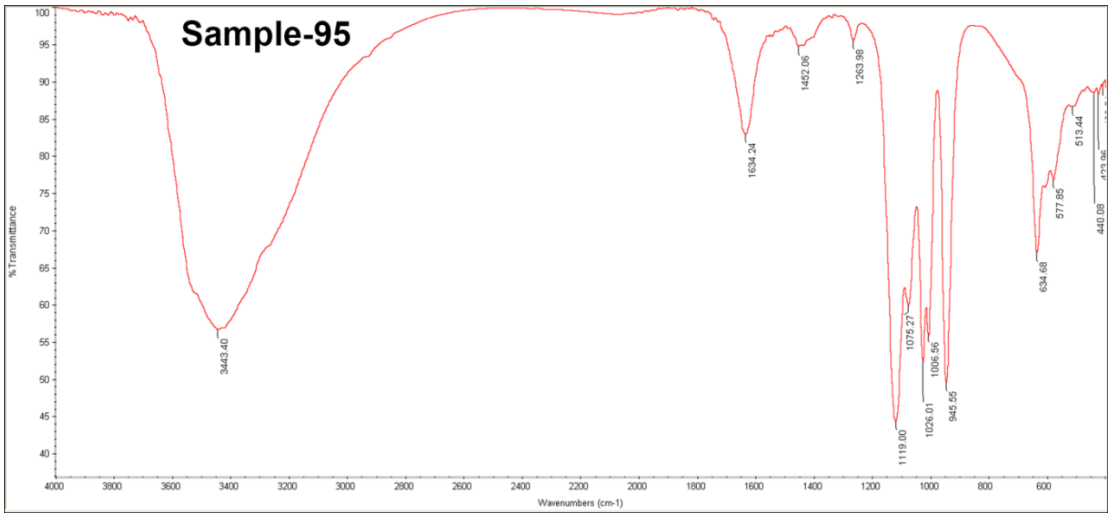

Fig. S9. The detailed FTIR spectra of the seven HZnPPs samples synthesized at 0~95 °C. All the absorbance peaks are illustrated in the picture one by one.

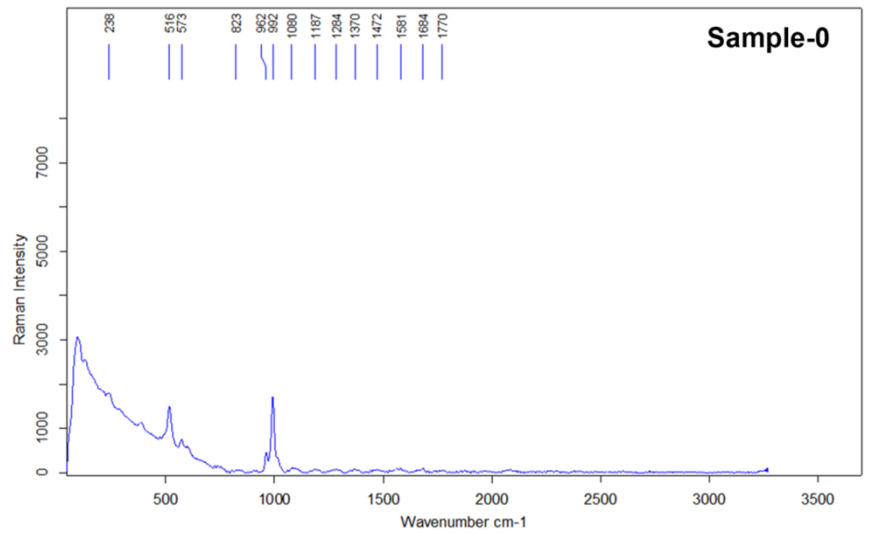

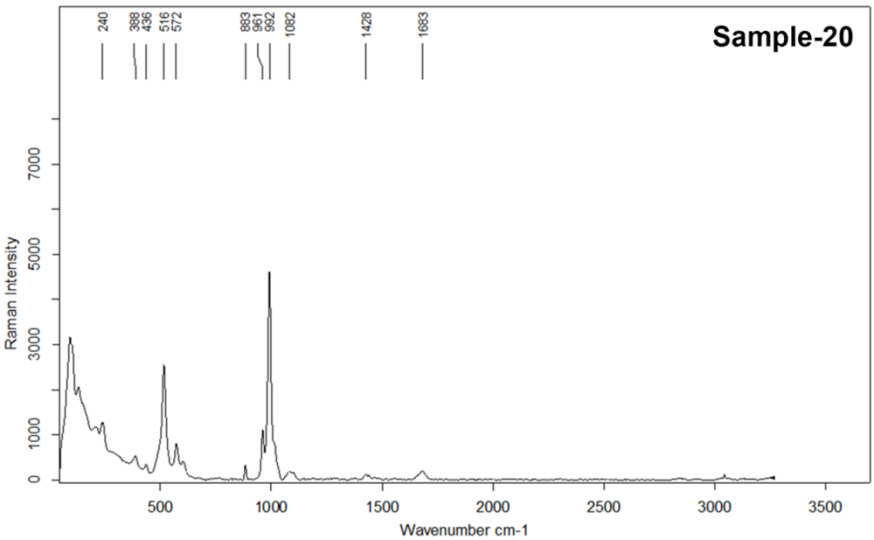

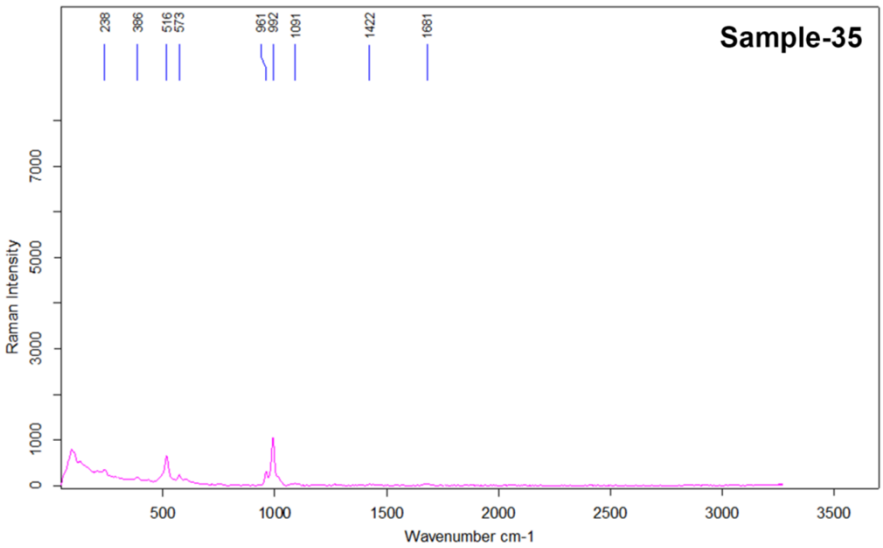
Sample-35
238
386
516
573
961
992
1091
1422
1681
Raman Intensity
0
1000
3000
5000
7000
500
1000
1500
2000
2500
3000
3500
Wavenumber cm-1

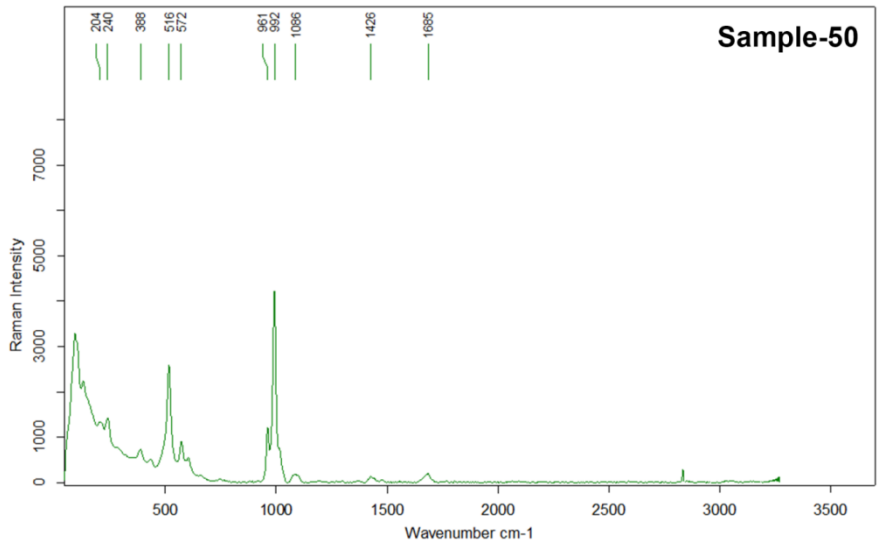
Sample-50
204
240
388
516
572
961
992
1086
1426
1685
Raman Intensity
0
1000
3000
5000
7000
500
1000
1500
2000
2500
3000
3500
Wavenumber cm-1

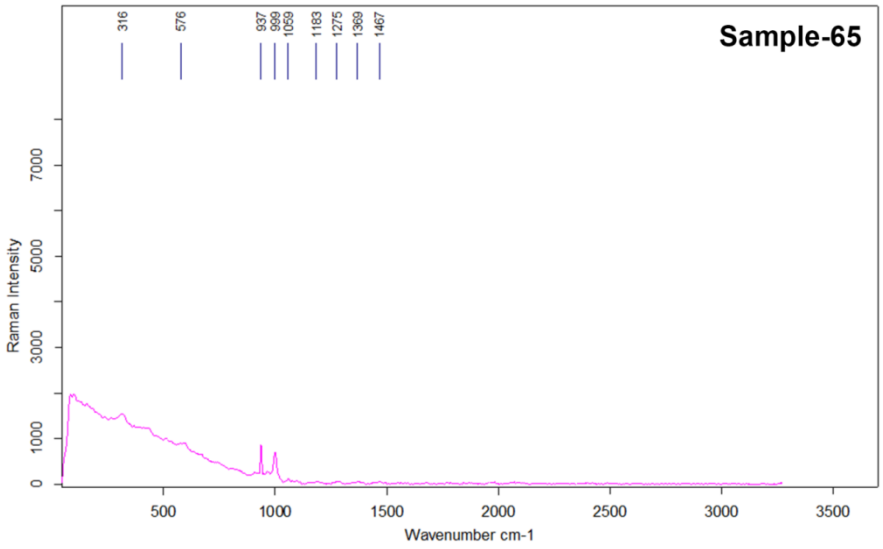
Sample-65
316
576
937
999
1059
1183
1275
1369
1467
Raman Intensity
0
1000
3000
5000
7000
500
1000
1500
2000
2500
3000
3500
Wavenumber cm-1

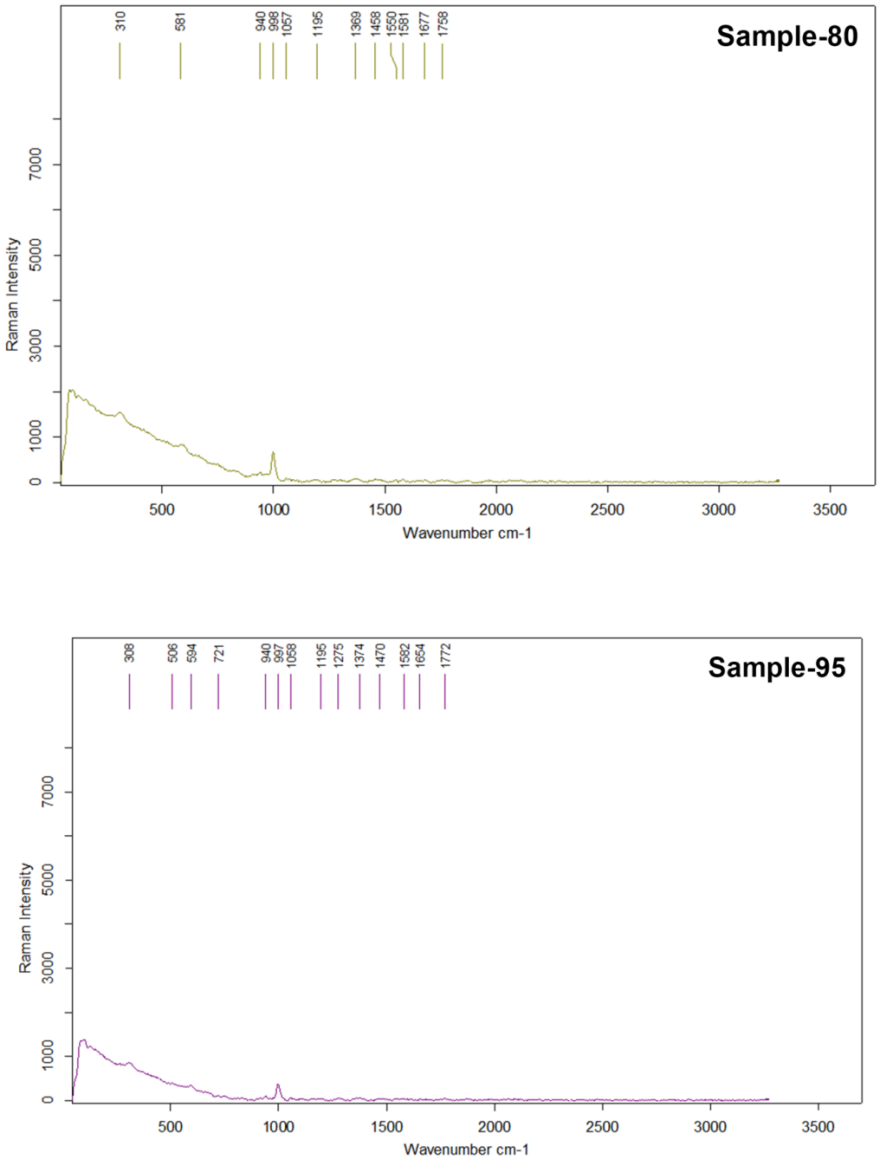

Fig. S10. The detailed Raman spectra of the seven HZnPPs samples synthesized at 0~95 °C. All the absorbance peaks are illustrated in the picture one by one.

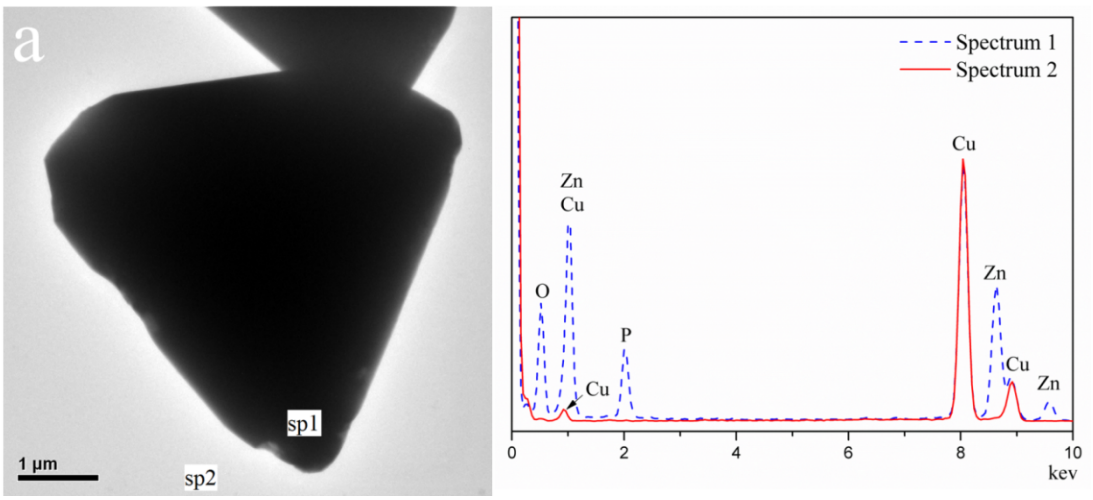
a
sp1
sp2
1 μm
Spectrum 1
Spectrum 2
Zn
Cu
O
P
Cu
Cu
Zn
Cu
Zn
0
2
4
6
8
10
kev

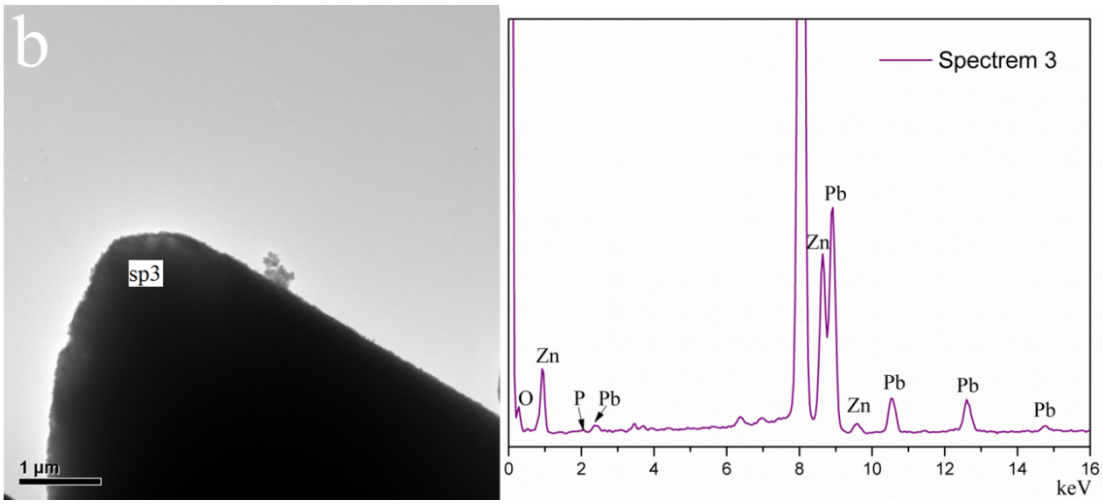
b
sp3
1 μm
Spectrem 3
Pb
Zn
Zn
O
P
Pb
Zn
Pb
Pb
Pb
0
2
4
6
8
10
12
14
16
keV

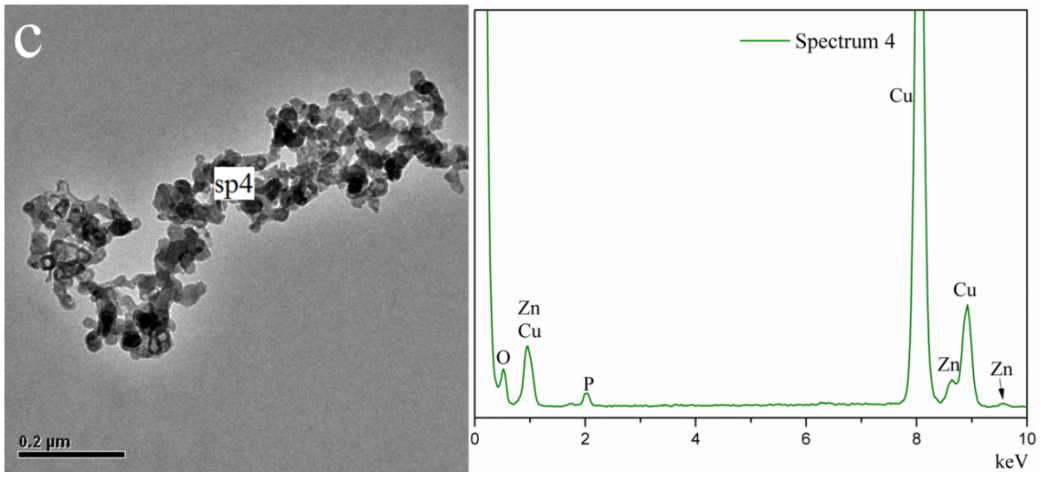
c
sp4
0.2 μm
Spectrum 4
Cu
Zn
Cu
O
P
Cu
Zn
Zn
0
2
4
6
8
10
keV

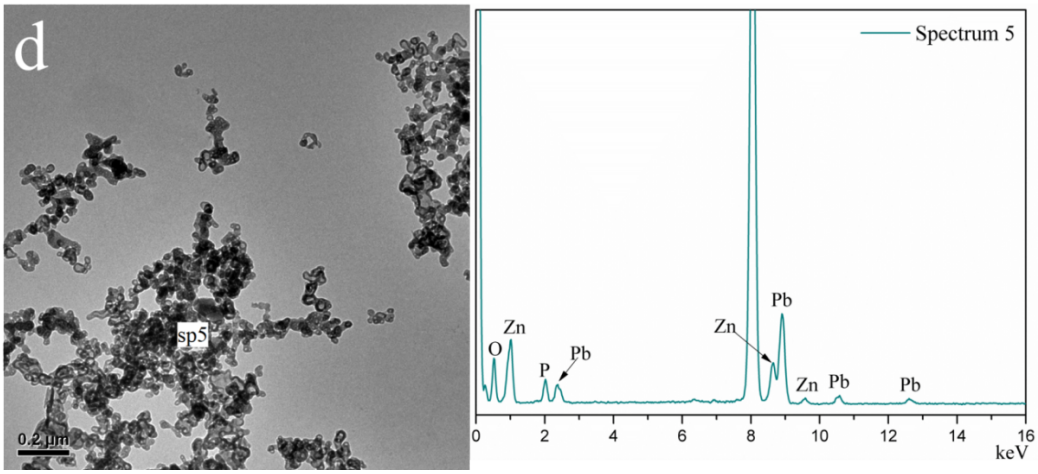

Fig. S11. The TEM obervation and corresponding with EDS analysis of (a) Cu^{2+}-adsorbed HZnPPs synthesized at 95 °C; (b) Pb^{2+} -adsorbed HZnPPs synthesized at 95 °C; (c) Cu^{2+}-adsorbed HZnPPs synthesized at 20 °C; (d) Pb^{2+} -adsorbed HZnPPs synthesized at 20 °C.

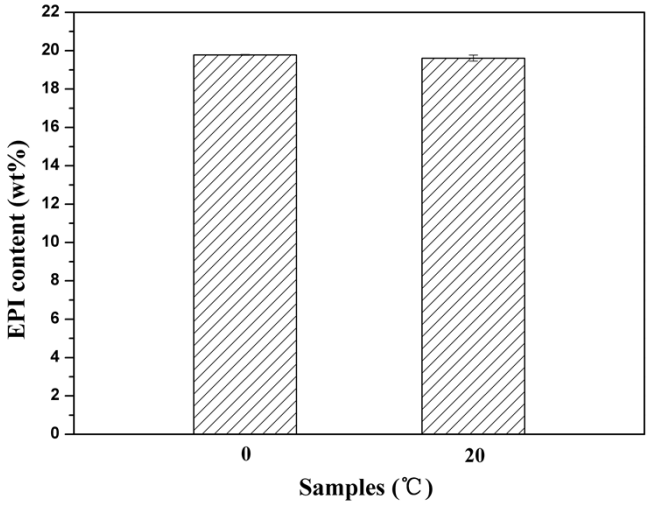

Fig.S12. Drug loading content (DLC) of EPI by the HZnPPs synthesized at 0 and 20 °C.